A Conservatism-Free Large Signal Stability Analysis Method for DC Microgrid Based on Mixed Potential Theory

Jianbo Jiang, Fei Liu, *Member, IEEE*, Shangzhi Pan, *Senior Member, IEEE*, Xiaoming Zha, *Member, IEEE*, Wenjun Liu, *Student Member, IEEE*, Chao Chen, and Lidong Hao

***Abstract*—Large disturbance scenarios, such as pulse power load operation and load switching are commonly seen in the operation of dc microgrids. The mixed potential theory-based large-signal stability (LSS) analysis is a simple and practical method for investigating the LSS of dc microgrids. However, this method is characterized by conservatism, and produces conservative stability criterion results. When they are applied to the parameter designs of dc microgrids, they create excessive control parameter redundancies; when used for running status estimations, they may cause the system to be misjudged as unstable, and trigger unnecessary protective actions when the system runs into the conservative region. This paper presents a comprehensive analysis of the conservatism, revealing its main causes to be the idealization of the load converter's response characteristics, and the lack of refined models. It then proposes a novel, improved analysis method for transient response characteristics of the load converter. Experimental and simulation results using the improved method have validated it by showing that the conservatism of the traditional method had been eliminated, and the stability criterion obtained was more accurate.**

***Index Terms*—Conservatism, dc microgrid, large signal stability(LSS), mixed potential theory(MPT), stability criterion.**

I. Introduction

IN ORDER to address the problem of environmental deterioration and the depletion of traditional fossil fuel energy, dc microgrids, with their advantage in seamless integration of distributed energy resources into utility grids, have drawn the attention of researchers in academia and the industry [1]. As of now, dc microgrids have been widely used in the fields of ship [2], electric vehicles [3], data center [4], household [5], and aircraft [6]. With the rapid development of microgrid applications, a large number of distributed energy resources have been integrated into utility grids indirectly, and in many cases, user loads are powered by the grid via power electronic converters

Manuscript received September 30, 2018; revised December 16, 2018; accepted January 26, 2019. Date of publication February 5, 2019; date of current version August 29, 2019. This work was supported in part by the National Natural Science Foundation of China under Grant 51637007. Recommended for publication by Associate Editor A. Davoudi. *(Corresponding author: Fei Liu.)*

The authors are with the School of Electrical Engineering, Wuhan University, Wuhan 430072, China (e-mail:

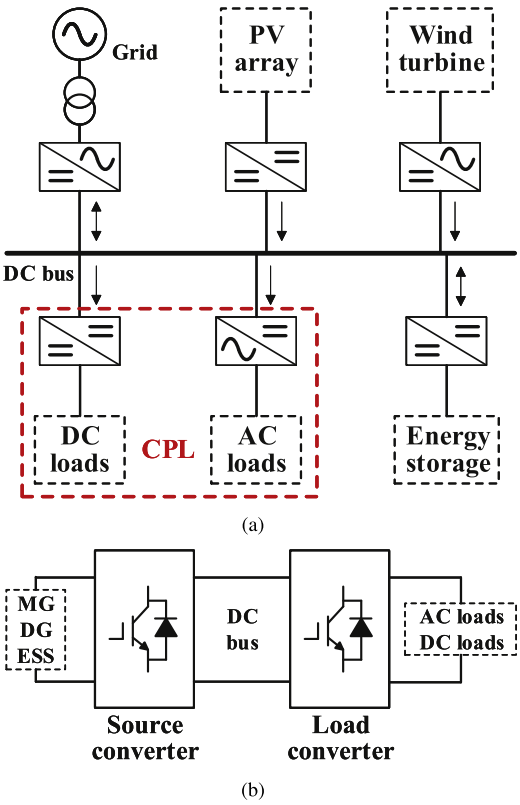

Fig. 1. Diagram of a typical dc microgrid. (a) Architecture. (b) Basic form.

approximations [17], but does not account for the influence of controller parameters on system stability. In addition, none of the five methods can provide a stability criterion in analytic form that covers both circuit and controller parameters. For instance, Lyapunov direct method and Hamiltonian surface shaping method can only provide a circuit parameter based stability criterion. Mixed potential theory, by contrast, is a more suitable tool for LSS analysis of dc microgrid, for it can provide a stability criterion in analytic form and this criterion involve both circuit parameters and controller parameters, useful for researchers in further investigations and improvements.

Since Brayton and Moser first proposed MPT [14], there had been follow-up studies devoted to the LSS analysis of dc power systems. Belkhayat *et al.* [18] developed a design-oriented MPT-based criterion for dc distributed systems with CPL to ensure LSS. [19]–[21] applied LSS analysis to aircraft power systems with CPL, each study obtained a stability criterion using MPT, and the ROA of system is determined by LaSalle invariance principle [20], [21]. Liu *et al.* [22]–[24] proposed design guidelines for various types of *LC* filters based on MPT. The generally accepted dc microgrid architecture usually consists of a common dc bus, a wind turbine system, a photovoltaic system, a grid-integrated converter, an energy storage system, and an ac and/or dc loads system, as shown in Fig. 1(a) [25]. These subsystems are all connected to the common dc bus via their respective converters. As a consequence, the studies above [18]–[24] are not suitable for dc microgrids because they all described CPL powered by the dc power source, whereas the CPL in dc microgrids are powered by source converters. There had also been studies on LSS for CPL powered by source converter. Du *et al.* [12] utilized MPT for LSS analysis on a cascaded system; while the method proved valid, the source converter utilized a traditional compensation circuit, as opposed to a digital controller, which has been increasingly widespread [26], [27]. Huang *et al.* [28] investigated the LSS of photovoltaic-battery hybrid power systems based on MPT, and obtained the LSS boundaries of circuit and controller parameters, but the accuracy of the boundaries had not been verified. In [7], the LSS of three-phase voltage source converters under grid voltage dips was examined based on MPT, and the conservatism of the obtained LSS boundaries was verified, but further study on conservatism of boundaries has not been carried out.

A common feature of the above findings is that all stability boundaries obtained via MPT had been characterized by conservatism, and this issue has yet to be addressed. Adherence to a conservative stability criterion gives a strong guarantee on the stability of the system. However, when using such conservative stability criterion as the guideline for dc microgrid designs, the need to preserve margins during the design process will require greater redundancies in control parameters. Too many redundancies will make the overall system closer to a first-order inertial system, at the cost of the source converter's response speed. Moreover, when the microgrid's operation monitoring is based on the conservative criterion, it is possible for the system to be misjudged as unstable and trigger protective actions when load power is still in an acceptable range. Therefore, in order to improve the accuracy of MPT-based stability analysis, and develop more reliable dc microgrids, there is a great need to find the primary causes of the MPT method's conservatism, and investigate approaches to eliminate it.

To address the issue, this paper starts by reviewing previous results of MPT-based analysis, and finds that they had all simplified the model by treating the loads with related converters as CPL. However, it is obvious that the transient responses of converter-powered loads under large disturbances differ from those of the ideal CPL, which means stability conclusions derived from the simplified model may deviate from reality. Based on this, an improved MPT-based method is proposed that accounts for the transient characteristics of the load converter to eliminate the conservatism of original method.

The remaining of the paper is organized as follows. Section II presents the system being studied, and derives the detailed mathematical model based on state space average method for each converter. Section III introduces the stability theorem of MPT, and derives the system's LSS criterion based on the traditional MPT method. Section IV analyzes the causes of conservatism in the preceding method, and proposes an improved MPT-based approach to LSS analysis. Experimental verifications are provided in Section V. Finally, the conclusion of this paper is given in Section VI.

II. Model Description

Since the concept of dc microgrid was proposed, different kinds of topologies have been derived. A typical topology of a dc microgrid is shown in Fig. 1(a). A dc bus is used to facilitate energy interaction between the main grid (MG), the distributed

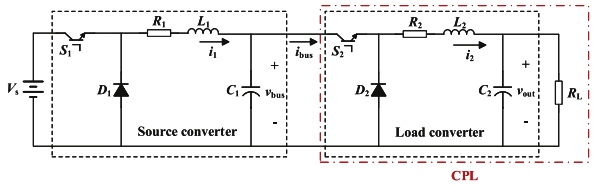

Fig. 2. Diagram of a cascaded system.

TABLE I
CASCADED SYSTEM PARAMETERS

Parameters	Value
ESS output voltage $V_{\rm s}$	100 V
Source converter inductance L_1	0.9 mH
Parasitic resistance R_1	20 mΩ
Source converter filter capacitor C_1	1 mF
Source converter voltage loop proportional coefficient $k_{\rm Svp}$	0.2
Source converter voltage loop integration coefficient $k_{\rm Svi}$	25
Source converter current loop proportional coefficient $k_{\rm Sip}$	0.1
Source converter current loop integration coefficient $k_{\rm Sii}$	10
Rated DC bus voltage $V_{\rm busref}$	50 V
Load converter inductance L_2	0.8 mH
Parasitic resistance R_2	15 mΩ
Load converter filter capacitor C_2	0.47 mF
Load converter voltage loop proportional coefficient $k_{\rm Lvp}$	0.2
Load converter voltage loop integration coefficient $k_{\rm Lvi}$	25
Load converter current loop proportional coefficient $k_{\rm Lip}$	0.1
Load converter current loop integration coefficient $k_{\rm Lii}$	10
Load converter rated output voltage $V_{\rm outref}$	30 V

generation system (DG), loads and the energy storage system (ESS). Fig. 1(b) shows the most basic form of dc microgrid, consisting of a source converter, a load converter and a dc bus.

A dc microgrid can operate under grid-connected or off-grid modes, and its MG, DG, and ESS also have different control modes, such as master–slave or droop control mode. For example, when a dc microgrid operates under the grid-connected mode with MG as the master source in master–slave control, the grid-integrated converter will be the source converter, and the remaining converters will the load converter. On the other hand, in a dc microgrid under off-grid droop control, the converters for DG and ESS will be regarded as the source converter, with the rest as the load converter. Therefore, the stability of cascaded converter systems can be used as a basis for investigating the overall stability of dc microgrids [12]. Without loss of generality, this paper examines a cascaded system with ESS as its power source. The diagram of studied system is shown in Fig. 2, which consist of two Buck converters, one as the source converter and the other as the load converter. The parameters of the cascaded system are summarized in Table I. Based on the state space averaging method, the source and load converters can be respectively modeled by (1) and (2).

$$\begin{cases} L_1 \dfrac{di_1}{dt} = d_1 V_{\rm s} - R_1 i_1 - v_{\rm bus} \\ C_1 \dfrac{dv_{\rm bus}}{dt} = i_1 - i_{\rm bus} \end{cases} \tag{1}$$

$$\begin{cases} L_2 \dfrac{di_2}{dt} = d_2 v_{\rm bus} - R_2 i_2 - v_{\rm out} \\ C_2 \dfrac{dv_{\rm out}}{dt} = i_2 - \dfrac{v_{\rm out}}{R_{\rm L}} \end{cases} \tag{2}$$

where d_1 and d_2 are duty cycles of the modulating signals of S_1 and S_2 respectively. The LSS analysis will be performed in the following sections.

III. Traditional LSS Criterion Based On MPT

The MPT was first put forward in 1964 [14], when it was used to investigate the stability of nonlinear circuits, before it was applied to power electronic systems. It can provide the LSS criterion in analytic form for estimating stability boundaries, which is convenient for designers and researchers. In this section, the MPT with its related stability theorem is introduced, and the LSS criterion of the studied system is obtained via the traditional method.

A. Introduction to the MPT

Based on Kirchhoff's law, the differential equation of a nonlinear circuit can be expressed as follows:

$$\begin{cases} L \dfrac{di_\rho}{dt} = \dfrac{\partial P(i,v)}{\partial i_\rho} \\ C \dfrac{dv_\sigma}{dt} = -\dfrac{\partial P(i,v)}{\partial v_\sigma} \end{cases} \tag{3}$$

where i_ρ are current of inductors and v_σ are voltage of capacitors. $P(i,v)$ refers to the mixed potential function which is a Lyapunov type energy function [12]. The mixed potential function can be expressed as follows:

$$P(i,v) = \int \sum_{\mu > r+s} v_\mu di_\mu + \sum_{\sigma=r+1}^{r+s} i_\sigma v_\sigma \tag{4}$$

where r is the number of inductor branches and s is the number of capacitor branches. The procedures for constructing the mixed potential function can be performed according to (4) as follows:

1) Calculate the current potential function of all non-energy storage element branches.
2) Calculate the product of current and voltage for all capacitor branches.
3) Add up the two items above.

Then, the unified form of mixed potential function is obtained as follows:

$$P(i,v) = -A(i) + B(v) + (i, \gamma v - \alpha) \tag{5}$$

where $A(i)$ is the current potential function, $B(v)$ is the voltage potential function, γ is a circuit structure-related constant matrix, and α is a constant vector. There are three related stability theorems for the LSS of nonlinear circuits in MPT. Since the current potential function is linear in the first stability theorem, and the voltage potential function is linear in the second one, neither are suitable for the studied system. Thus the third stability theorem is adopted, as defined below.

If $\mu_1 + \mu_2 \geq \delta, \delta > 0$ for all i, v and

$$P^*(i,v) = \left(\frac{\mu_1 - \mu_2}{2}\right) P(i,v) + \frac{1}{2}\left(P_i, L^{-1} P_i\right) + \frac{1}{2}\left(P_v, C^{-1} P_v\right) \to \infty \tag{6}$$

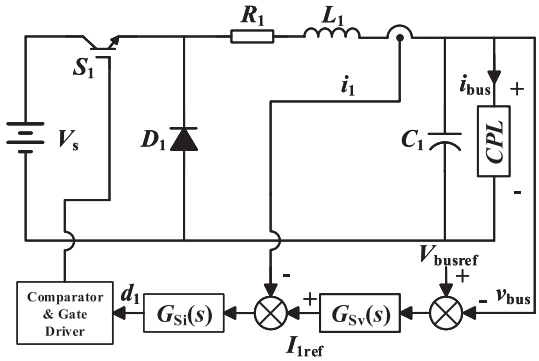

Fig. 3. Diagram of cascaded system and control scheme.

as $|i|+|v|\to\infty$, then all solutions of the studied system approach the equilibrium solutions as $t\to\infty$ [14]. Where μ_1 is the minimum eigenvalue of $L^{-1/2}A_{ii}(i)L^{-1/2}$ and μ_2 is the minimum eigenvalue of $C^{-1/2}B_{vv}(v)C^{-1/2}$, $P_i=\partial P(i,v)/\partial i$, $P_v=\partial P(i,v)/\partial v$, $A_{ii}(i)=\partial^2 A(i)/\partial i^2$, $B_{vv}(v)=\partial^2 B(v)/\partial v^2$.

B. Estimation of LSS Boundaries

The LSS boundary for a cascaded system is estimated in this section based on MPT. Traditional LSS method (hereinafter traditional method) usually simplifies the load converter into a CPL. Therefore, the cascaded system shown in Fig. 2 can be simplified into the model in Fig. 3. This paper applies the voltage and current double closed-loop controlling method to source converter because the widely accepted fact is that the performance of double closed-loop scheme is better than voltage single close-loop scheme. Besides, we adopt the digital PI controller in cascaded system to regulate the control parameters flexibly.

As shown in Fig. 3, the load converter has been simplified to a CPL, and its current response can be described as $i_{\rm bus}=P_{\rm L}/v_{\rm bus}$, where $P_{\rm L}$ is load power, $G_{\rm Sv}(s)=k_{\rm Svp}+k_{\rm Svi}/s$, $G_{\rm Si}(s)=k_{\rm Sip}+k_{\rm Sii}/s$; $k_{\rm Svp}$ and $k_{\rm Svi}$ are respectively the proportionality and integration coefficient of the outer voltage loop of the source converter, $k_{\rm Sip}$ and $k_{\rm Sii}$ are respectively the proportionality and integration coefficient of the inner current loop of the source converter. According to Fig. 3, the model of control system of source converter is obtained as

$$\begin{cases} I_{1\rm ref}=k_{\rm Svp}(V_{\rm busref}-v_{\rm bus})+k_{\rm Svi}\int(V_{\rm busref}-v_{\rm bus})\,dt \\ d_1=k_{\rm Sip}(I_{1\rm ref}-i_1)+k_{\rm Sii}\int(I_{1\rm ref}-i_1)\,dt \end{cases} \tag{7}$$

where the parameters of controller are the same as those presented in Table I.

The source converter has the feature of controlled current source because a current inner loop controller exists in the source converter. The CPL current will change in the opposite direction when a voltage dip or swell occurs in the supply side, which will intensify the voltage fluctuation further, hence the CPL can also be equivalent to a controlled current source. Therefore, the cascaded system can be simplified as the circuit shown in Fig. 4.

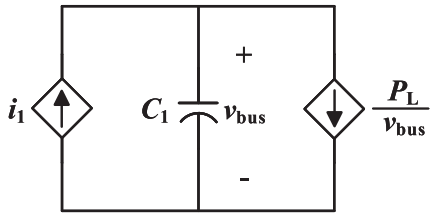

Fig. 4. Equivalent circuit of cascaded system.

Combined with the equivalent circuit and the aforementioned procedures, the mixed potential function of cascaded system can be written as

$$\begin{aligned} P(i,v) &= \int_0^{i_1} v_{\rm bus}di_1-\int_0^{i_{\rm bus}}\frac{P_{\rm L}}{i_{\rm bus}}di_{\rm bus}+v_{\rm bus}(i_{\rm bus}-i_1) \\ &= -\int_0^{v_{\rm bus}} i_1 dv_{\rm bus}+\int_0^{v_{\rm bus}}\frac{P_{\rm L}}{v_{\rm bus}}dv_{\rm bus}. \end{aligned} \tag{8}$$

The correctness of the obtained mixed potential function can be verified when (8) is introduced into (3)

$$\frac{\partial P(i,v)}{\partial v_{\rm bus}}=-i_1+\frac{P_{\rm L}}{v_{\rm bus}}=-C_1\frac{dv_{\rm bus}}{dt}. \tag{9}$$

Then, the obtained mixed potential function can be converted to a uniform expression as shown in (5) to achieve the following equation set:

$$\begin{cases} A(i)=0 \\ B(v)=-\int_0^{v_{\rm bus}} i_1 dv_{\rm bus}+\int_0^{v_{\rm bus}}\frac{P_{\rm L}}{v_{\rm bus}}dv_{\rm bus} \\ (i,\gamma v-\alpha)=0 \end{cases}. \tag{10}$$

According to the third stability theorem of MPT

$$\begin{cases} A_{ii}=0 \\ B_{vv}=-\dfrac{\partial i_1}{\partial v_{\rm bus}}-\dfrac{P_{\rm L}}{v_{\rm bus}^2} \end{cases}. \tag{11}$$

Solving the differential equation shown in the first term of (1) results in

$$i_1=\frac{d_1V_{\rm s}-v_{\rm bus}}{R_1}-f(t) \tag{12}$$

where $f(t)$ is a time-varying item ($f(t)=\frac{N}{R_1}e^{-R_1t/L_1}$, N is a constant value) and has no effect on the results of partial differentiation. Then, the partial differentiation item of (11) can be obtained combining (7) and (12)

$$\frac{\partial i_1}{\partial u_{\rm bus}}=-\frac{V_{\rm s}k_{\rm Sip}k_{\rm Svp}}{R_1+V_{\rm s}k_{\rm Sip}}. \tag{13}$$

Finally, when $|i_1|+|v_{\rm bus}|\to\infty$, we have $P^*(i,v)\to\infty$. Therefore, the LSS criterion of cascaded system is obtained from (11), (13), and $\mu_1+\mu_2>0$, which can be written as

$$\begin{cases} \dfrac{V_{\rm s}k_{\rm Sip}k_{\rm Svp}}{R_1+V_{\rm s}k_{\rm Sip}}>\dfrac{P_{\rm L}}{V_{\rm busref}^2} \\ P_{\rm L}<P_{\rm batN} \end{cases} \tag{14}$$

where $P_{\rm batN}$ is the rated discharge power of ESS.

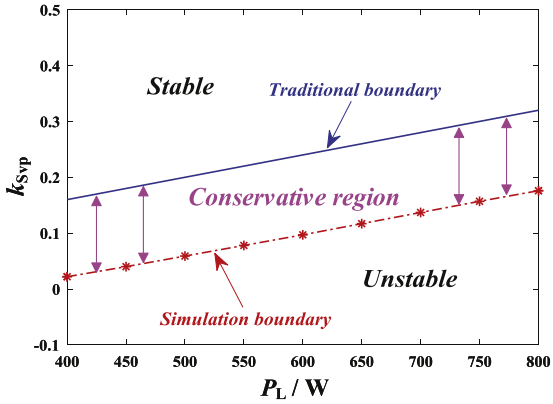

Fig. 5. LSS boundaries for cascaded system.

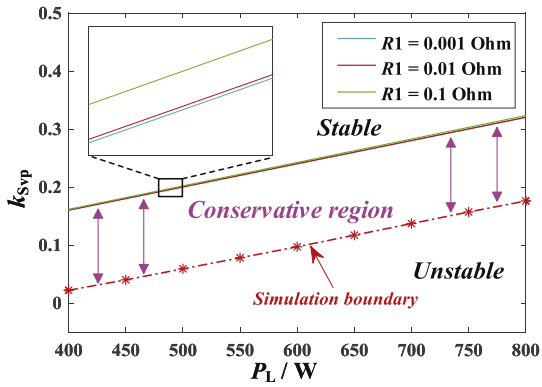

Fig. 6. Stability boundaries under different converter internal resistances.

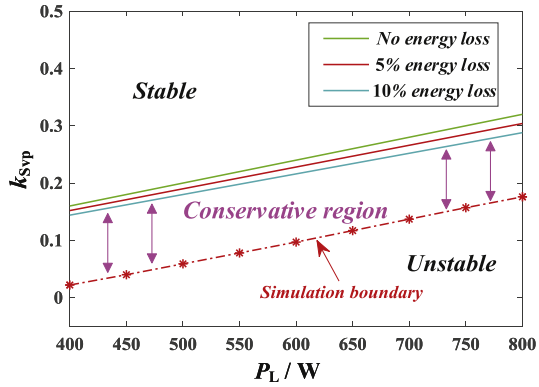

Fig. 7. Stability boundaries under different converter energy losses.

The key parameters that affect the LSS of cascaded system is obtained from (14) mainly consist of $P_{\rm L}$ and $k_{\rm Svp}$. However, this does not mean other parameters have no effect on the stability of the cascaded system. For instance, the phase margin at the crossing frequency will be decreased accompany the increase of $k_{\rm Sip}$, but $k_{\rm Sip}$ cannot be too low, or otherwise the actual current will be unable to keep up with the reference current [28].

The LSS boundary for the cascaded system is obtained from (14) is shown by the solid line in Fig. 5. A simulation model is established using MATLAB/Simulink, and the parameters of the system are the same as those provided in Table I. All the simulation work in this paper is based on this simulation model. The LSS boundary of the simulation system is obtained by trial and error, as shown by the dotted line in Fig. 5, and red asterisk dots represent the points of stability boundary which have been verified by simulation. Compared with the stability boundary of simulation model, it is salient that the boundary obtained by the traditional method is characterized by conservatism.

IV. MPT Based Improved Method

The hazards of conservatism have been elaborated in Section I. This section starts with a comprehensive exploration for why conservatism exists in the traditional method. Then, an improved method of LSS analysis, based on MPT, is proposed (hereinafter improved method).

A. Investigation for Causes of Conservatism

In order to find the causes of conservatism in the traditional method, the entire process, from the establishment of the mathematical model, to the derivation of the stability boundary, needs to be thoroughly investigated. The potential causes of conservatism include parasitic parameters and the modeling method.

First of all, in terms of parasitic parameters, the internal resistance and energy loss of the converter is not taken into consideration during the analysis process. When the internal resistance is incorporated into the parasitic resistance R_1 for (14), the influence of converter internal resistance on the stability boundary can be found, shown in Fig. 6. The energy loss can also be incorporated into load power $P_{\rm L}$ for (14), and its influence is shown in Fig. 7. It can be seen from Figs. 6 and 7 that the internal resistance and energy loss of the converter have little effect on the stability boundary. Therefore, neither are the key source for conservatism.

We then take a look at the modeling methods. The state space averaging method is applied to establish the mathematical model of the cascaded system. However, the accuracy of this method has already been verified, meaning it is not the cause. Finally, an assumption which considers the load converter as an ideal CPL is frequently used to simplify the model. It can be seen from (14) that the nature of the MPT-based LSS criterion is that when the bus voltage fluctuates, the system will be stable if the change rate of the source converter's output current relative to the bus voltage exceeds that of the load converter's input current relative to the bus voltage. However, the actual load converter's responses are significantly slower than those of the ideal CPL when a large disturbance occurs in the system as shown in Fig. 8. Therefore, compared with the actual load, the ideal CPL will cause the value of the first item on the right side of (14) to be larger than actual one, thereby introducing the problem of conservatism. From this point of view, the assumption that treats the load converter as an ideal CPL is the main cause of conservatism, and an improved method can therefore be developed.

B. Improved Method for LSS Analysis

In order to address the problem of conservatism, this paper proposes an improved method for LSS analysis, which analyzes

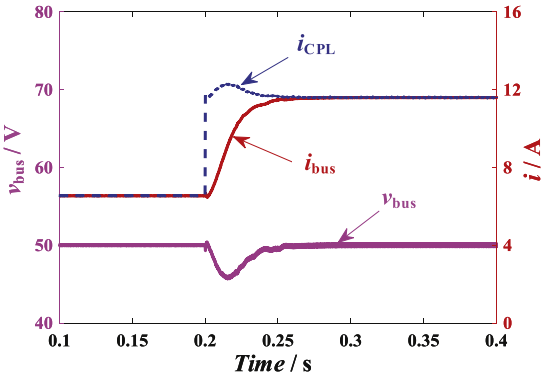

Fig. 8. Voltage and current waveform under large disturbance.

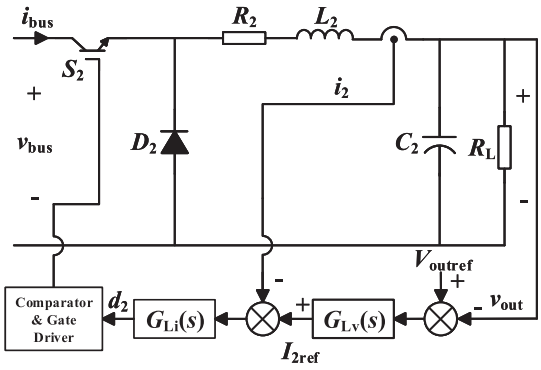

Fig. 9. Diagram of load converter and control scheme.

the transient response characteristics of the load converter under bus voltage fluctuations from the input side. First the large signal mathematical model needs to be established to analyze the transient response characteristics of load converter. The diagram of load converter is shown as Fig. 9. And the load converter adopts the voltage and current double closed-loop controlling method as well.

As shown in Fig. 9, $G_{\mathrm{Lv}}(s) = k_{\mathrm{Lvp}} + k_{\mathrm{Lvi}}/s$, $G_{\mathrm{Li}}(s) = k_{\mathrm{Lip}} + k_{\mathrm{Lii}}/s$, k_{Lvp} and k_{Lii} is proportionality and integration coefficient of outer voltage loop of load converter, k_{Lip} and k_{Lii} is proportionality and integration coefficient of inner current loop of load converter. According to Fig. 9, the model of control system of load converter is obtained as

$$\begin{cases} I_{2\mathrm{ref}} = k_{\mathrm{Lvp}}\left(V_{\mathrm{outref}} - v_{\mathrm{out}}\right) + k_{\mathrm{Lvi}}\int\left(V_{\mathrm{outref}} - v_{\mathrm{out}}\right)dt \\ d_2 = k_{\mathrm{Lip}}\left(I_{2\mathrm{ref}} - i_2\right) + k_{\mathrm{Lii}}\int\left(I_{2\mathrm{ref}} - i_2\right)dt \end{cases} \tag{15}$$

where the parameters of controller are the same as those listed in Table I and the value of R_{L} is obtained by $R_{\mathrm{L}} = V_{\mathrm{outref}}^2/P_{\mathrm{L}}$.

As mentioned before, the source converter can be equivalent to a controlled current source, the load converter can also be equivalent to a controlled current source because the current inner loop controller exists in control system. Therefore, the cascaded system can be simplified to the circuit shown in Fig. 10.

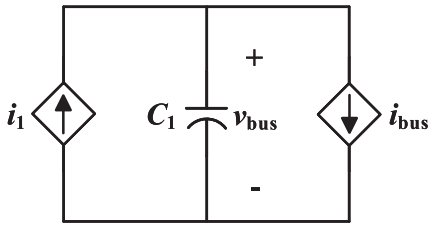

Fig. 10. Equivalent circuit of cascaded system.

So, the mixed potential function can be written as

$$\begin{cases} A(i) = 0 \\ B(v) = -\int_0^{v_{\mathrm{bus}}} i_1 dv_{\mathrm{bus}} + \int_0^{v_{\mathrm{bus}}} i_{\mathrm{bus}} dv_{\mathrm{bus}} \\ (i, \gamma v - \alpha) = 0. \end{cases} \tag{16}$$

According to third stability theorem of MPT,

$$\begin{cases} A_{ii} = 0 \\ B_{vv} = -\dfrac{\partial i_1}{\partial v_{\mathrm{bus}}} + \dfrac{\partial i_{\mathrm{bus}}}{\partial v_{\mathrm{bus}}}. \end{cases} \tag{17}$$

In order to derive the change rate of input current of load converter relative to the bus voltage, first, the differential equation shown in the first term of (2) is solved

$$i_2 = \frac{d_2 v_{\mathrm{bus}} - v_{\mathrm{out}} - f_1(t)}{R_2} \tag{18}$$

where $f_1(t) = Ne^{-R_2 t/L_2}$ is a time-varying item. Then, combine

$$i_2 = \frac{k_{\mathrm{Lip}} I_{2\mathrm{ref}} v_{\mathrm{bus}} - v_{\mathrm{out}} + f_2(t)}{R_2 + k_{\mathrm{Lip}} v_{\mathrm{bus}}} \tag{19}$$

where $f_2(t) = k_{\mathrm{Lii}}\int\left(I_{2\mathrm{ref}} - i_2\right)dt - f_1(t)$ is a time-varying item and has no effect on the results of partial differentiation. Ignore the energy loss of the load converter to get $i_{\mathrm{bus}} v_{\mathrm{bus}} = i_2 v_{\mathrm{out}}$, so,

$$i_{\mathrm{bus}} = \frac{v_{\mathrm{out}} i_2}{v_{\mathrm{bus}}} = \frac{k_{\mathrm{Lip}} I_{2\mathrm{ref}} v_{\mathrm{bus}} v_{\mathrm{out}} - v_{\mathrm{out}}^2 + v_{\mathrm{out}} f_2(t)}{R_2 v_{\mathrm{bus}} + k_{\mathrm{Lip}} v_{\mathrm{bus}}^2} \tag{20}$$

Now, from (13), (17), (20), and $\mu_1 + \mu_2 > 0$

$$\frac{\left(R_2 + 2k_{\mathrm{Lip}} v_{\mathrm{bus}}\right)\left(v_{\mathrm{out}}^2 - k_{\mathrm{Lip}} I_{2\mathrm{ref}} v_{\mathrm{out}} v_{\mathrm{bus}}\right)}{\left(k_{\mathrm{Lip}} v_{\mathrm{bus}}^2 + R_2 v_{\mathrm{bus}}\right)^2} + \frac{V_{\mathrm{s}} k_{\mathrm{Sip}} k_{\mathrm{Svp}}}{R_1 + V_{\mathrm{s}} k_{\mathrm{Sip}}} + \frac{k_{\mathrm{Lip}} I_{2\mathrm{ref}} v_{\mathrm{out}}}{k_{\mathrm{Lip}} v_{\mathrm{bus}}^2 + R_2 v_{\mathrm{bus}}} > 0. \tag{21}$$

In the steady state, $P_{\mathrm{L}} = I_{2\mathrm{ref}} v_{\mathrm{out}}$ can be obtained, so the LSS criterion of cascaded system can be written as

$$\begin{cases} \dfrac{\left(R_2 + 2k_{\mathrm{Lip}} V_{\mathrm{busref}}\right)\left(V_{\mathrm{outref}}^2 - k_{\mathrm{Lip}} P_{\mathrm{L}} V_{\mathrm{busref}}\right)}{\left(k_{\mathrm{Lip}} V_{\mathrm{busref}}^2 + R_2 V_{\mathrm{busref}}\right)^2} \\ + \dfrac{V_{\mathrm{s}} k_{\mathrm{Sip}} k_{\mathrm{Svp}}}{R_1 + V_{\mathrm{s}} k_{\mathrm{Sip}}} + \dfrac{k_{\mathrm{Lip}} P_{\mathrm{L}}}{k_{\mathrm{Lip}} V_{\mathrm{busref}}^2 + R_2 V_{\mathrm{busref}}} > 0 \\ P_{\mathrm{L}} < P_{\mathrm{batN}}. \end{cases} \tag{22}$$

Improved LSS boundary for cascaded system is obtained from as shown by the black curve in Fig. 11. It can be seen from

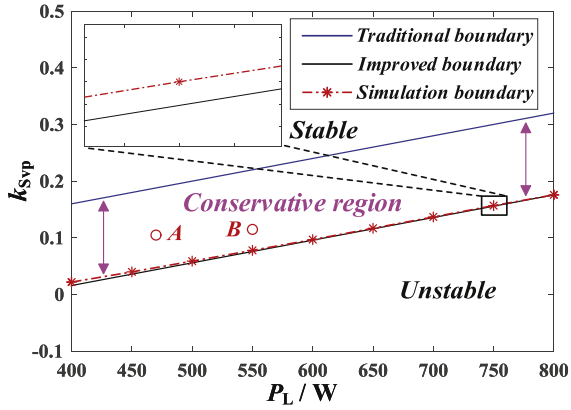

Fig. 11. LSS boundaries for cascaded system.

Fig. 11 that the stability boundary obtained by the improved method almost coincides with the simulation boundary.

Based on MPT, a novel analysis method for transient response characteristic of load converter is proposed in this paper and it is applied to the LSS analysis of dc microgrid. The transient response characteristics of load converter are modeled from input side instead of regarding the load converter as ideal CPL in the traditional method. Compared with traditional method, the accurate lLSS boundary of dc microgrid can be obtained by proposed method and thereby eliminating the conservative issue existing in original method. The analysis process of proposed method is simple and easy to conduct, and can provide reference for parameter design of a power electronics dominated dc power system. The accuracy of the improved method will be verified experimentally in the next section.

V. Simulation And Experimental Verification

To verify the conservatism of traditional method and the validity of the improved method, an experimental system with two Buck converters is developed, one for simulating the source converter and the other for simulating the load converter and both of them adopting voltage and current double closed-loop controlling scheme. Since the trial-and-error method is used to determine the stability boundary of the system, it is inevitable to carry out some experiments under unstable operating situations. Therefore, it is necessary to configure the limiter at the output of every voltage outer loop to ensure that the converter is not damaged by overvoltage or overcurrent. The system parameters are shown as Table I. A Chroma 62100H-600S programmable power source is utilized to simulate the ESS in the system. Fig. 12 shows the experimental diagram of studied system.

A. Verification for Conservatism of the Traditional Method

In order to verify the conservatism of the traditional method, two groups of parameters are used for simulation and experiment, where one group define $k_{\mathrm{Svp}} = 0.105$ and load power step up from 250 to 470 W and shown as point A ($k_{\mathrm{Svp}} = 0.105, P_{\mathrm{L}} = 470$ W) in Fig. 11. Another group define $k_{\mathrm{Svp}} = 0.115$ and load power step up from 250 to 550 W and shown as point B ($k_{\mathrm{Svp}} = 0.115, P_{\mathrm{L}} = 550$ W) in Fig. 11. Ac-

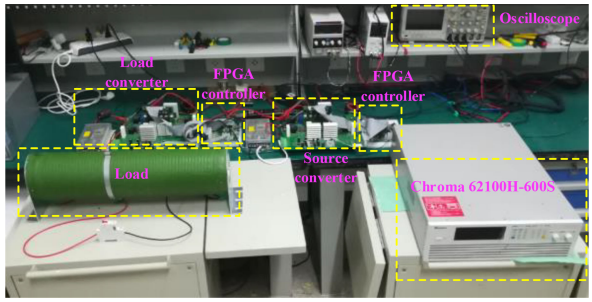

Fig. 12. Experimental diagram.

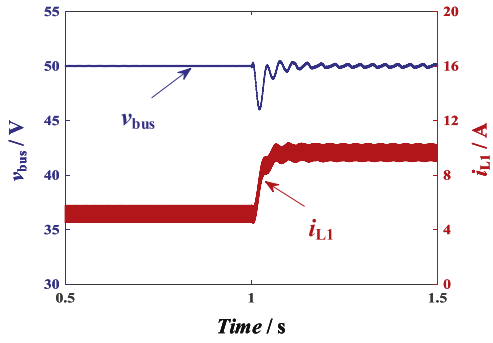

(a)

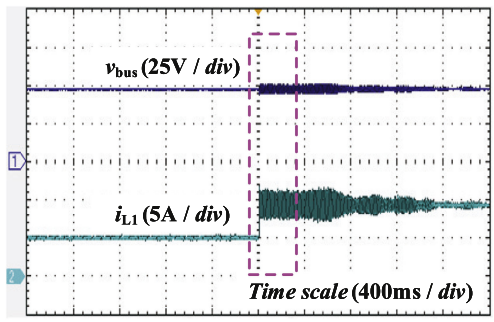

(b)

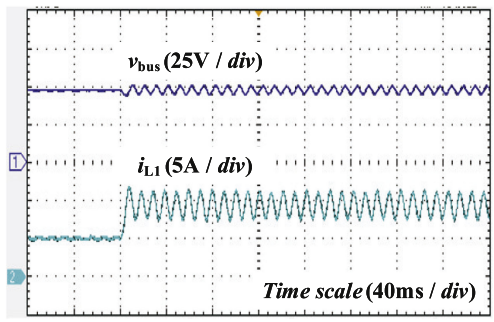

(c)

Fig. 13. Waveforms of dc bus voltage and inductance current of source converter. (a) Simulation result of the first group of parameters. (b) Experimental result of the first group of parameters. (c) Enlarged waveform of (b).

cording to traditional method, two groups of parameters given in above are exceed the stability boundary obtained by traditional method and the system will be operating in unstable status. Fig. 13 shows the results of simulation and experiment when the system adopts first group of parameters, Fig. 14 shows the results of simulation and experiment when the system adopts

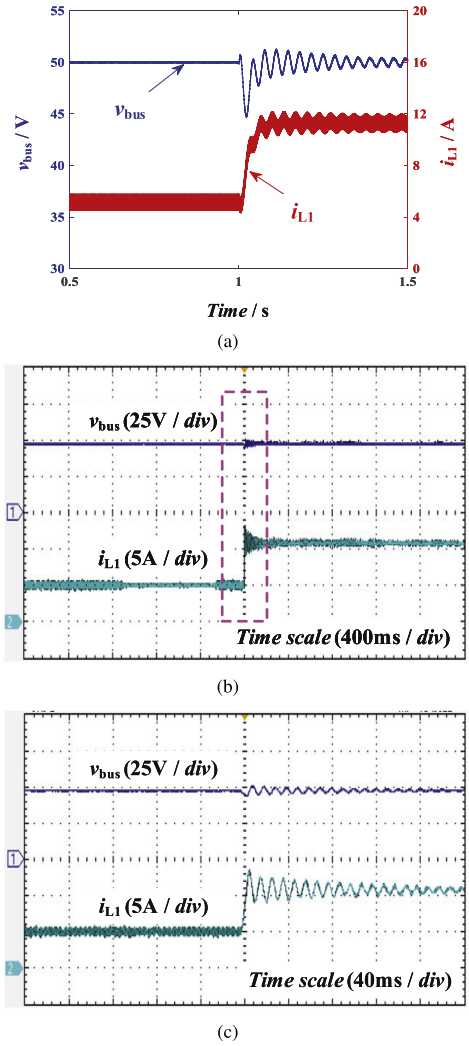

Fig. 14. Waveforms of dc bus voltage and inductance current of source converter. (a) Simulation result of the second group of parameters. (b) Experimental result of the second group of parameters. (c) Enlarged waveform of (b).

second group of parameters. It is obvious that the system is stable no matter which group of parameters is used. Therefore, the conservatism of traditional method has been verified.

B. Verification for Validity of Improved Method

A trial-and-error method was adopted to experiment on obtaining the actual boundaries. The initial load power was set to 250 W in all experiments and simulations. Fig. 15 shows the respective stability boundaries obtained by the traditional and the improved methods, simulation, and experiment. As can be seen from Fig. 15, compared with the traditional stability boundary, the improved stability boundary is closer to actual results, which validates the improved method. The slight discrepancy between the improved boundary and experimental boundary is mainly caused by parasitic loss of load converter and error of signal acquisition system. The forward voltage of IGBT ($V_{ce} = 1.8$ V) is taken into account in the simulation model to investigate the influence of parasitic loss on simulation boundary, and the corresponding simulation results are shown by the green dashed

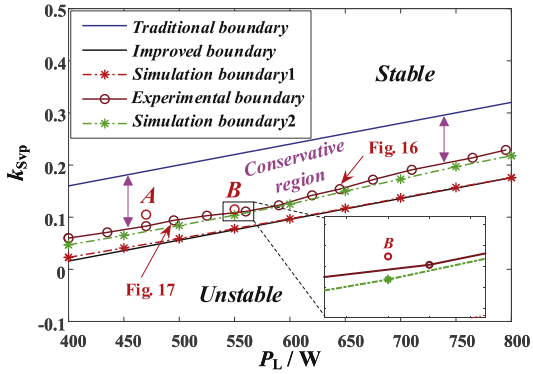

Fig. 15. Stability boundaries from various methods: Traditional method, improved method, simulation verification without parasitic parameters, experimental verification, and simulation verification with parasitic parameters.

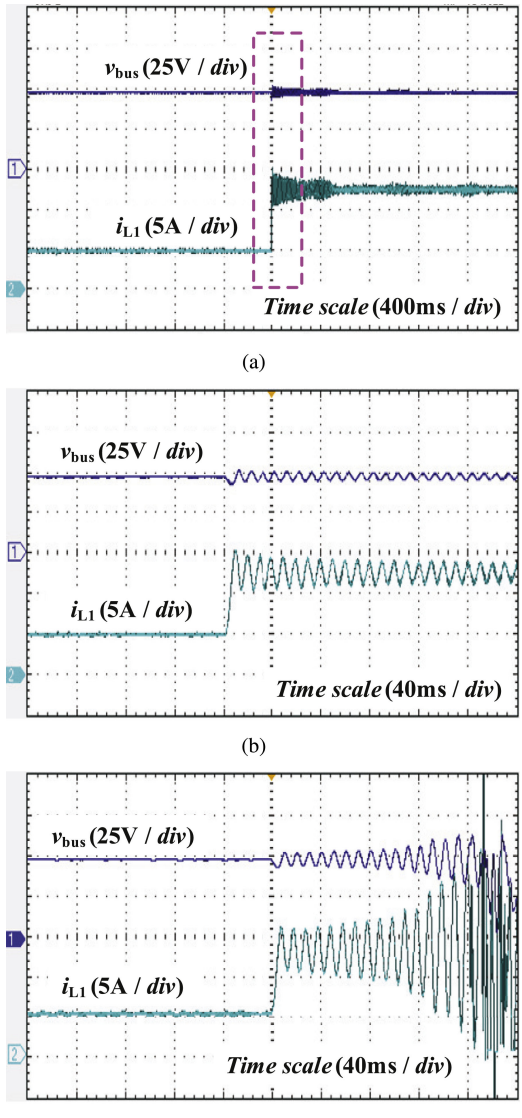

Fig. 16. Experimental verification of the improved method. (a) Waveforms of dc bus voltage and inductance current of source converter at the test point ($k_{Svp} = 0.154, P_L = 645$ W) in the experimental boundary. (b) Enlarged waveform of (a). (c) DC bus voltage and current waveforms at the test point ($k_{Svp} = 0.153, P_L = 645$ W) outside the stable zone.

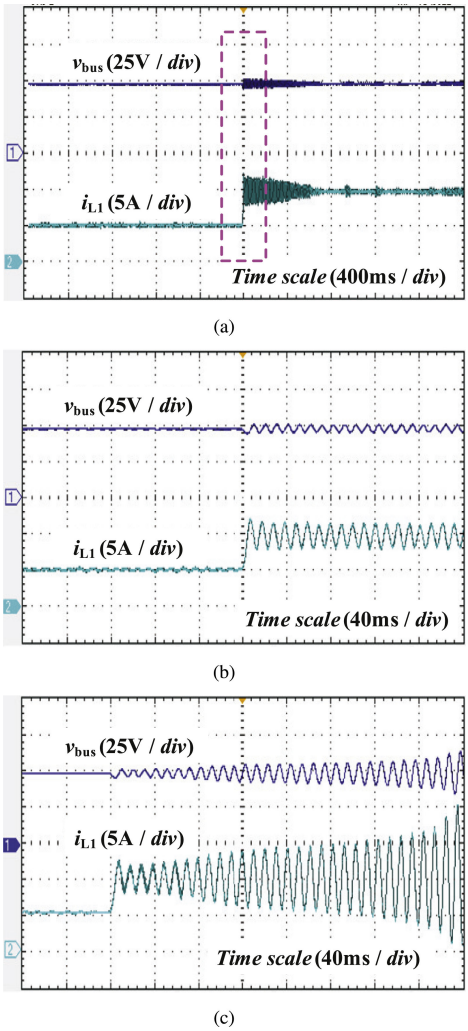

Fig. 17. Experimental verification of the improved method. (a) Waveforms of dc bus voltage and inductance current of source converter at the test point ($k_{\mathrm{Svp}} = 0.094, P_{\mathrm{L}} = 495$ W) in the experimental boundary. (b) Enlarged waveform of (a). (c) DC bus voltage and current waveforms at the test point ($k_{\mathrm{Svp}} = 0.093, P_{\mathrm{L}} = 495$ W) outside the stable zone.

TABLE II
CASCADED SYSTEM PARAMETERS

k_{Svp}	P_{L}	k_{Svp}	P_{L}
0.060	400 W	0.142	620 W
0.071	435 W	0.154	645 W
0.083	470 W	0.172	675 W
0.094	495 W	0.191	710 W
0.103	525 W	0.214	765 W
0.111	560 W	0.229	795 W
0.123	590 W		

line in Fig. 15, which is closer to experimental boundary, while the simulation results without considering the forward voltage are represented by the red dashed line. It is proved that the parasitic loss is the main reason leading to the discrepancy between the improved boundary and the experimental boundary. Two sets of experimental results near stability boundary are shown in Figs. 16 and 17. Data of test points on the experimental boundary are shown in Table II.

VI. CONCLUSION

In this paper, an improved LSS analysis method, based on the MPT, is proposed to address the conservatism of the traditional method. The LSS of the studied system was first analyzed by the traditional MPT-based method, and the obtained stability criterion was found to be conservative. The nature of this conservatism was then analyzed, revealing the most important causes to be the idealization of the load converter's response characteristics, and the lack of refined models. By analyzing the transient response characteristics of the load converter under bus voltage fluctuations, a stability criterion without conservatism was obtained. Simulations and experiments were conducted on a cascaded system with two buck converters, verifying the conservatism of traditional method and the validity of the improved method. This improved method is applicable to power electronics-dominated dc power system where multiple converters are cascaded or connected in parallel, and complexity of analysis will increase proportionally as the number of converters increases.

REFERENCES

[1] M. Kabalan, P. Singh, and D. Niebur, "Large signal lyapunov-based stability studies in microgrids: A review," *IEEE Trans. Smart Grid*, vol. 8, no. 5, pp. 2287–2295, Sep. 2017.
[2] G. Sulligoi, D. Bosich, G. Giadrossi, L. Zhu, M. Cupelli, and A. Monti, "Multiconverter medium voltage dc power systems on ships: Constant-power loads instability solution using linearization via state feedback control," *IEEE Trans. Smart Grid*, vol. 5, no. 5, pp. 2543–2552, Sep. 2014.
[3] A. Emadi, A. Khaligh, C. H. Rivetta, and G. A. Williamson, "Constant power loads and negative impedance instability in automotive systems: Definition, modeling, stability, and control of power electronic converters and motor drives," *IEEE Trans. Veh. Technol.*, vol. 55, no. 4, pp. 1112–1125, Jul. 2006.
[4] Y. Hayashi, H. Toyoda, T. Ise, and A. Matsumoto, "Contactless dc connector based on GAN LLC converter for next-generation data centers," *IEEE Trans. Ind. Appl.*, vol. 51, no. 4, pp. 3244–3253, Jul. 2015.
[5] A. Chub, D. Vinnikov, E. Liivik, and T. Jalakas, "Multiphase quasi-Z-source dc– dc converters for residential distributed generation systems," *IEEE Trans. Ind. Electron.*, vol. 65, no. 10, pp. 8361–8371, Oct. 2018.
[6] J. S. Ngoua Teu Magambo *et al.*, "Planar magnetic components in more electric aircraft: Review of technology and key parameters for dc– dc power electronic converter," *IEEE Trans. Transp. Electrific.*, vol. 3, no. 4, pp. 831–842, Dec. 2017.
[7] M. Huang, Y. Peng, C. K. Tse, Y. Liu, J. Sun, and X. Zha, "Bifurcation and large-signal stability analysis of three-phase voltage source converter under grid voltage dips," *IEEE Trans. Power Electron.*, vol. 32, no. 11, pp. 8868–8879, Nov. 2017.
[8] Y. Gu, W. Li, and X. He, "Passivity-based control of dc microgrid for self-disciplined stabilization," *IEEE Trans. Power Syst.*, vol. 30, no. 5, pp. 2623–2632, Sep. 2015.
[9] T. Dragievi, X. Lu, J. C. Vasquez, and J. M. Guerrero, "DC microgrids part 1: A review of control strategies and stabilization techniques," *IEEE Trans. Power Electron.*, vol. 31, no. 7, pp. 4876–4891, Jul. 2016.
[10] M. Amin and M. Molinas, "Small-signal stability assessment of power electronics based power systems: A discussion of impedance- and eigenvalue-based methods," *IEEE Trans. Ind. Appl.*, vol. 53, no. 5, pp. 5014–5030, Sep. 2017.
[11] H. Kim, S. Kang, G. Seo, P. Jang, and B. Cho, "Large-signal stability analysis of dc power system with shunt active damper," *IEEE Trans. Ind. Electron.*, vol. 63, no. 10, pp. 6270–6280, Oct. 2016.
[12] W. Du, J. Zhang, Y. Zhang, and Z. Qian, "Stability criterion for cascaded system with constant power load," *IEEE Trans. Power Electron.*, vol. 28, no. 4, pp. 1843–1851, Apr. 2013.
[13] D. Marx, P. Magne, B. Nahid-Mobarakeh, S. Pierfederici, and B. Davat, "Large signal stability analysis tools in dc power systems with constant power loads and variable power loads: A review," *IEEE Trans. Power Electron.*, vol. 27, no. 4, pp. 1773–1787, Apr. 2012.

[14] R. K Brayton and J. K Moser, "A theory of nonlinear networks. I, II," *Quart. Appl. Math*, vol. 2, no. 2, pp. 1–33, Apr. 1964.
[15] B. P. Loop, S. D. Sudhoff, S. H. Zak, and E. L. Zivi, "Estimating regions of asymptotic stability of power electronics systems using genetic algorithms," *IEEE Trans. Control Syst. Technol.*, vol. 18, no. 5, pp. 1011–1022, Sep. 2010.
[16] A. Bacha, H. Jerbi, and N. B. Braiek, "An approach of asymptotic stability domain estimation of discrete polynomial systems," in *Proc. Multiconf. Comput. Eng. Syst. Appl.*, 2006, vol. 1, pp. 288–292.
[17] W. W. Weaver, R. D. Robinett, D. G. Wilson, and R. C. Matthews, "Metastability of pulse power loads using the hamiltonian surface shaping method," *IEEE Trans. Energy Convers.*, vol. 32, no. 2, pp. 820–828, Jun. 2017.
[18] M. Belkhayat, R. Cooley, and A. Witulski, "Large signal stability criteria for distributed systems with constant power loads," in *Proc. Power Electron. Specialist Conf.*, 1995, vol. 2, pp. 1333–1338.
[19] Y. Che, J. Xu, K. Shi, H. Liu, W. Chen, and D. Yu, "Stability analysis of aircraft power systems based on a unified large signal model," *Energies*, vol. 10, no. 11, 2017, Art. no. 1739.
[20] A. Griffo and J. Wang, "Large signal stability analysis of 'more electric' aircraft power systems with constant power loads," *IEEE Trans. Aerosp. Electron. Syst.*, vol. 48, no. 1, pp. 477–489, Jan. 2012.
[21] A. Griffo, J. Wang, and D. Howe, "Large signal stability analysis of dc power systems with constant power loads," in *Proc. IEEE Veh. Power Propulsion Conf.*, 2008, pp. 1–6.
[22] X. Liu and S. Ma, "Large signal stabilization method of constant power loads by adding r parallel damping filters," in *Proc. IEEE Energy Convers. Congr. Expo.*, pp. 1314–1319, Sep. 2015.
[23] X. Liu, S. Ma, Z. Li, and N. Wang, "Large signal stability analysis for constant power loads with RC parallel damping filters," in *Proc. 17th Int. Conf. Elect. Mach. Syst.*, 2014, pp. 2796–2801.
[24] X. Liu, Y. Zhou, W. Zhang, and S. Ma, "Stability criteria for constant power loads with multistage LC filters," *IEEE Trans. Veh. Technol.*, vol. 60, no. 5, pp. 2042–2049, Jun. 2011.
[25] T. Dragievi, X. Lu, J. C. Vasquez, and J. M. Guerrero, "DC microgrids Part—II: A review of power architectures, applications, and standardization issues," *IEEE Trans. Power Electron.*, vol. 31, no. 5, pp. 3528–3549, May 2016.
[26] J. A. Abu Qahouq and V. Arikatla, "Online closed-loop autotuning digital controller for switching power converters," *IEEE Trans. Ind. Electron.*, vol. 60, no. 5, pp. 1747–1758, May 2013.
[27] M. Shirazi, R. Zane, and D. Maksimovic, "An autotuning digital controller for dc– dc power converters based on online frequency-response measurement," *IEEE Trans. Power Electron.*, vol. 24, no. 11, pp. 2578–2588, Nov. 2009.
[28] M. Huang, H. Ji, J. Sun, L. Wei, and X. Zha, "Bifurcation-based stability analysis of photovoltaic-battery hybrid power system," *IEEE J. Emerg. Sel. Topics Power Electron.*, vol. 5, no. 3, pp. 1055–1067, Sep. 2017.

Jianbo Jiang was born in Baoshan, Yunnan Province, China, in 1992. He received the B.S. and M.S. degrees from Yunnan University, Kunming, China, in 2014 and 2017, respectively. He is currently working toward the Ph.D. degree in electrical engineering at Wuhan University, Wuhan, China.

His research interests include transient stability of dc microgrid and the topology and control of photovoltaic inverter.

Fei Liu (M'14) was born in Hanchuan, Hubei Province, China, in 1977. He received the B.S., M.S., and Ph.D. degrees from the Huazhong University of Science and Technology, Wuhan, China, in 2000, 2004, and 2008, respectively.

He has been a Faculty Member with Wuhan University since 2010, and is currently working as an Associate Professor with the School of Electrical Engineering, Wuhan University, Wuhan, China. His research interests include dc microgrid, cascaded multi-level converter, and interface of utility-scale photovoltaic conversion systems.

Shangzhi Pan (M'08–SM'14) received the B.Sc. and M.Sc. degrees in electrical engineering from Zhejiang University, China, in 1998 and 2001, respectively, and the Ph.D. degree from Queen's University, Kingston, ON, Canada in 2008.

He joined the College of Electrical Engineering, Wuhan University, China in 2018, where he is currently a Professor. He is also an Adjunct Faculty at the Queen's Center of Energy and Power Electronics Applied Research Laboratory (ePOWER) since 2014. Previously he worked as the VP of research and development at SPARQ Systems, a Queen's Spun-off photovoltaic microinverter company since 2010. He was a Senior Research Engineer at Queen's University from 2008 to 2013. His research interests include digital control techniques for power converters, grid-connected inverters, voltage regulators for computing systems, power converters for renewable energy sources, and power converters for electric vehicles.

Xiaoming Zha (M'02) was born in Huaining, Anhui Province, China, in 1967. He received the B.S., M.S., and Ph.D. degrees in electrical engineering from Wuhan University, Wuhan, China, in 1989, 1992, and 2001, respectively.

He was a Postdoctoral Fellow in the University of Alberta, Canada from 2001 to 2003. He has been a Faculty Member with Wuhan University since 1992, and became a Professor in 2003. He is now the Deputy Dean with the School of Electrical Engineering, Wuhan University, Wuhan, China. His research interests include power electronic converter, the application of power electronics in smart grid and renewable energy generation, the analysis and control of microgrid, the analysis and control of power quality, and frequency control of high-voltage high-power electric motors.

Wenjun Liu (S'16) was born in Zhengzhou, Henan Province, China, in 1990. She received the B.S. degree in electrical engineering from Wuhan University, Wuhan, China, in 2013. She is currently working toward the Ph.D. degree in electrical engineering at Wuhan University, Wuhan, China.

Her research interests include cascaded multi-level converter, the protection system of dc microgrid, and overvoltage protection device.

Chen Chao was born in Ningbo, Zhejiang Province, China, in 1993. He received the B.S. degree in electrical engineering from the Dalian University of Technology, Liaoning, China, in 2016. He is currently working toward the M.S. degree in electrical engineering at Wuhan University, Wuhan, China.

His research interests include the protection system and stability analysis of dc microgrid.

Lidong Hao was born in Handan, China, in 1987. He received the B.S. degree from the Hebei University of Technology City College, Tianjin, China, in 2013, and the M.S. degree from the Hebei University of Science and Technology, Shijiazhuang, China, in 2017. He is currently working toward the Ph.D. degree in electrical engineering at Wuhan University, Wuhan, China.

His research interests include transient stability of dc microgrid and high frequency dc–dc converters.